Biochimica et Biophysica Acta, 688 (1982) 75–87
Elsevier Biomedical Press

BBA 71132

LOW-TEMPERATURE STUDIES OF THE SARCOPLASMIC RETICULUM CALCIUM PUMP

MECHANISM OF CALCIUM BINDING

YVES DUPONT

Laboratoire de Biologie Moléculaire et Cellulaire (E.R. CNRS 199), Département de Recherche Fondamentale, Centre d'Etudes Nucléaires de Grenoble, 85X, 38041 Grenoble Cedex (France)

(Received June 1st, 1981)
(Revised manuscript received December 21st, 1981)

Key words: Ca^{2+}-ATPase; Ca^{2+} binding; Low-temperature study; Fluorescence spectroscopy; (Sarcoplasmic reticulum; Rabbit muscle)

The mechanism of the sarcoplasmic reticulum Ca^{2+}-ATPase was investigated at low temperatures (0 to −12°C). Transient states of the enzyme were studied by two complementary techniques: intrinsic protein fluorescence and rapid filtration on Millipore filters. Intrinsic fluorescence was used to distinguish conformational states of the protein and to evaluate the rate of conversion between these states. Filtrations were used to measure the evolution of the active sites during the transition; the time resolution was 2–5 s. At sub-zero temperatures this time is shorter than the lifetime of most of the enzymatic states which have been detected. In this paper the mechanism of Ca^{2+} binding to the protein is investigated in the absence of nucleotides. Two basic experiments are described; (1) Kinetics of calcium binding and dissociation over a wide range of calcium concentration. (2) Kinetics of calcium exchange ($^{45}Ca^{2+} \rightleftarrows {}^{40}Ca^{2+}$) at constant concentration. The results obtained in the first series of experiments are consistent with a sequential binding to two interacting Ca^{2+} binding sites. Calcium ions have very fast access to a site with low apparent affinity ($K_d \approx 25\ \mu M$). Occupation of this site induces a slow conformational change which increases its apparent affinity and reveals a second site of high apparent affinity. At equilibrium the two sites are not equivalent in terms of rate of exchange. Two different rates were detected $k_{fast} > 0.2\ s^{-1}$, $k_{slow} \approx 0.015\ s^{-1}$ at −10°C. Removal of Ca^{2+} from the fast exchanging site by addition of EGTA accelerates the rate of release of the slow exchanging one. A model is proposed with two interacting Ca^{2+}-binding sites. A set of parameters has been obtained which reproduces correctly the Ca^{2+}-binding curve and the fluorescence level at equilibrium as well as the rate constants of the calcium-induced fluorescence changes over a very wide range of Ca^{2+} concentrations (0.02 to 150 μM). The non-equivalence of the two classes of site and the meaning of the initial low-affinity binding are discussed.

Introduction

In order to understand the mechanism of calcium transport by the sarcoplasmic reticulum Ca^{2+} pump it is essential to identify and to characterize the intermediate states of the translocation process. In the past, most of the kinetic information has been obtained from measurements of phosphoryl-enzyme formation or decay; data on the unphosphorylated form have been derived only indirectly.

Recently a new method has been developed

Abbreviations: POPOP, 1,4-bis(5-phenyloxazolyl-2)-benzene; PPO, 2,5-diphenyloxazole; Mops, 4-morpholinepropanesulfonic acid.

0005-2736/82/0000–0000/$02.75 © 1982 Elsevier Biomedical Press

which uses the intrinsic fluorescence of the protein [1,4]. This technique offers the opportunity to follow the transitions between essential conformation states of the protein in the absence of phosphorylating substrates. Titration of active sites, however, can be achieved only with labeled compounds ($^{45}Ca^{2+}$, [γ-^{32}P]ATP or [^{14}C]ATP) and the fastest method of measurement, Millipore filtration, is usually too slow for kinetic experiments. However, as shown in this article, this is possible at subzero temperatures where the lifetimes of some important states of the Ca^{2+} pump are much longer than the time of filtration (usually 2–5 s).

Low temperature has been used in the study of a number of soluble enzymes [5] and it is shown here that it can also give unique information on membrane proteins through the complementary use of intrinsic fluorescence and filtration techniques.

This first article describes the study of the calcium binding and of the calcium induced conformational change at low temperature in the absence of nucleotides. This important step in the enzyme cycle has been investigated in earlier studies by direct $^{45}Ca^{2+}$ binding [6–12], by measurements of the calcium concentration dependence of the ATPase activity [1,13,14] or more recently by the study of the intrinsic fluorescence of the protein [1–4]. That two high-affinity sites are involved in the enzymatic cycle has been deduced mostly from the fact that two calcium ions are transported per ATP molecule cleaved. The nature of the interaction between these two sites, is however, as yet not solved. Cooperative calcium-dependent activation of the ATPase has been reported [13,15,16] but data on cooperative calcium binding are fewer [11,12]. Fast kinetic experiments using the calcium-induced intrinsic fluorescence changes have not, so far, led to any definite conclusion. The original experiments [2,4] were analysed in term of the simplest model: a two-state scheme associated with calcium binding to a single class of non-interacting sites, the affinity for calcium being different in the two conformations of the protein.

Recently Inesi et al. [11] have proposed a more refined interpreation of calcium binding and fluorescence data based on sequential binding to two high-affinity calcium sites.

In the present work the time course of the $^{45}Ca^{2+}$ binding release and exchange has been studied by filtration at sub-zero temperatures and compared with tryptophan fluorescence measurements in the same solvent and under the same temperature conditions.

Analysis of the kinetic and equilibrium data reveals clearly the existence of two interacting calcium sites. The first part of the present article is devoted to the description of experiments concerning the effect of low temperatures and organic solvents on the enzyme Ca^{2+}-ATPase.

Materials and Methods

Sarcoplasmic reticulum vesicles were prepared from rabbit muscle as described by Hasselbach and Makinose [17]. Additional details of the preparation and sample conservation can be found in Ref. 18. Protein concentration was determined by the folin method [34].

The equipment and the procedure used for filtration on Millipore filters (HAWP 0.45 μm) has been described in detail in a recent paper [6]. Kinetic experiments were always repeated without vesicles to measure the $^{45}Ca^{2+}$ background. The radioactivity of the filters was counted with a Nuclear Chicago Unilux II in a dioxane/PPO/POPOP scintillant.

Fluorescence experiments

Fluorescence measurements were made with a Durrum D117 stop-flow fluorimeter coupled to a Datalab transient recorder. Some measurements were made with the Durrum stop-flow equipment and a modified temperature regulation arrangement, but most of the data presented here were performed by replacing the standard observation chamber by a 1×1 cm fluorimeter cuvette stirred from the top by a propeller. The excitation was provided by a 75 W xenon (Hg) arc at 295 nm. The emitted light was collected at 90° through quartz lenses and filtered with an O-54 Corning filter coupled to a wide-band ultraviolet filter to eliminate ambient light. The resulting bandpass was 60 nm wide, centered at 355 nm with a peak transmission of 75%. The high efficiency of detection permitted the use of low-intensity emission light which resulted in a very low photolysis rate. Substrates were injected on the stirring propeller

with Hamilton microsyringes (CR-700-20) in very small volumes (1–10 μl) to prevent temperature changes and dilution artefacts.

pa_H measurements

The protonic activity of the solvent (pa_H) was measured in the mixed solvents with a standard pH meter by comparison with phosphate buffer in the same solvent. pa_H of phosphate was obtained from tabulated values [5].

The EGTA-Ca complex at low temperatures

The EGTA-Ca stability constant was evaluated at each temperature and for each solvent used, by measuring free Ca^{2+} and free EGTA in a test solution consisting of 100 mM KCl/1 mM Mops/1 mM EGTA/1 mM Ca^{2+}. Around neutral pH, 2 mol protons are released per mol EGTA-Ca complex formed [19]; free calcium in the test solution was determined by injection of 20 mM EGTA and free EGTA was determined separately by injection of 20 mM Ca^{2+}. The proton production was measured in a 10 ml thermostatically controlled cell with a TTT 1 Radiometer pH-Stat using 10 mM KOH as titrant.

Results are compiled in Table I and are compared with values calculated from [20].

At −10°C, 30% glycerol and $pa_H = 7.20$, this method yields a stability constant of $3.1 \cdot 10^6$ M^{-1}. This value was corrected for the effect of 5 mM Mg^{2+} as described in Ref. 21 and a constant of $2.5 \cdot 10^6$ M^{-1} was adopted and used throughout this work for calculating the free calcium concentration. This constant is strongly pa_H-dependent (Table I). Error bars in the data presented below were calculated assuming a reproducibility of pa_H measurement of ±0.05 pa_H units and including the uncertainties on the evaluation of the endogenous Ca^{2+}.

Association between Ca^{2+} and EGTA has been reported to be a relatively slow process [22]. Since kinetic experiments described in this article have always been initiated by a change in Ca^{2+} concentration produced by mixing Ca^{2+} with EGTA, a series of experiments was then designed to measure the overall dead time of this technique at −10°C and 30% glycerol. 10 μM Ca^{2+} was injected into the 2 ml fluorimeter cell containing 100 μM KCl, 1 mM Mops ($pa_H = 7.20$), 10–100 μM EGTA, 20 μM of the pH indicator bromcresol purple and 30% glycerol. The time course of the proton release produced by the EGTA-Ca association was followed at 595 nm. The absorption change observed was always complete in less than 1 s. This was found sufficiently fast for most of the fluorescence changes presented in this report. (Compare with the time course of the fluorescence experiment presented in Fig. 5.)

X-Ray diffraction

Measurement of the lipid phase transition was performed by X-ray diffraction on a membrane sample pelleted in the appropriate solvent. The apparatus is identical to that used by Davis et al. [23]. A standard with pure egg lecithin was used to mark the position of the sharp 4.2 Å reflection [23,24].

The X-ray generator was an Elliot GX6 and the

TABLE I

EGTA-Ca^{2+} STABILITY CONSTANTS

Measured as described in 'Methods' or calculated from Ref. 20. Stability constants are expressed in M^{-1} and all such values shown are multiplied by 10^{-6}.

Temperature (°C)	pa_H 7.00			pa_H 7.20		
	H_2O		30% glycerol (Measured)	H_2O		30% glycerol (Measured)
	Calculated	Measured		Calculated	Measured	
20	5	2.4	1.7	12	5.0	3.8
0	–	2.7	1.3	–	6.2	3.3
−10	–	–	1.0	–	–	3.1

detection was made with a position-sensitive proportional counter [25].

Results

(A) Preliminary study of solvents and temperature effects

Effect of solvents on the activity of the Ca^{2+} pump

The freezing temperatures of the various solvents tested are listed in the Table II. Two indicators of the calcium pump activity in these solvents were used: the ATPase activity and the coupling ratio (Ca^{2+} transported/ATP hydrolysed). The measurements were made at 20°C with a pH-stat as described in Ref. 18. Glycerol had a slight activating effect on the ATPase activity, while the coupling ratio was significantly decreased, this certainly reflected an effect of the solvent on the membrane permeability. It was also apparent that ethylene glycol/methanol mixtures might be interesting for temperatures below −10°C. Long-term solvent effects were also tested by overnight incubation at low temperature (above the freezing point) followed by heating at 20°C and measurement of ATPase activity and coupling ratio. There were no detectable differences with control samples freshly diluted in the same solvent.

Order-disorder transition in the sarcoplasmic reticulum membrane

The physical state of the membrane lipids is an important parameter which has to be taken into account for membrane enzymology at subzero temperatures. An abrupt change in the activation energy for the transport process has been reported to occur around 20°C. It has been suggested [26] that this change is produced by a change in the physical state of the membrane. According to Davis et al. [23] this transformation, however, does not involve a phase transition of the lipids, since they were not able to detect a 4.2 Å reflection in the X-ray diffraction pattern at a temperature as low as 1°C. These authors have nevertheless related the change in activation energy to a change in lipid molecular motion observed by NMR at the same temperature. To our knowledge, however, a thermal transition in the protein conformation or a change in rate-limiting step has not been com-

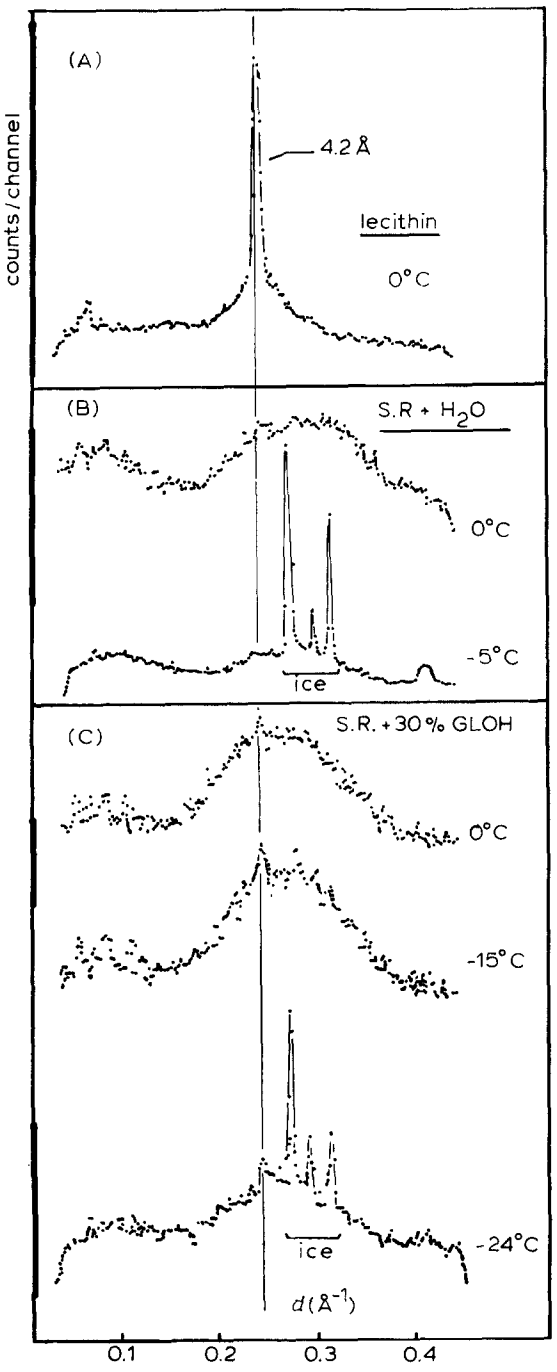

Fig. 1. High angle X-ray diffraction spectra of sarcoplasmic reticulum (S.R.) membrane. In water (B) or in 30% glycerol (GLOH) (C). As the temperature decreases a faint 4.2 Å reflection becomes visible. Spectra in ethylene glycol (not shown) were identical to those taken in glycerol. A spectrum with pure lecithin is shown to indicate the position of the 4.2 Å reflection (A). Bars on ordinates represent 10^3 counts/channel.

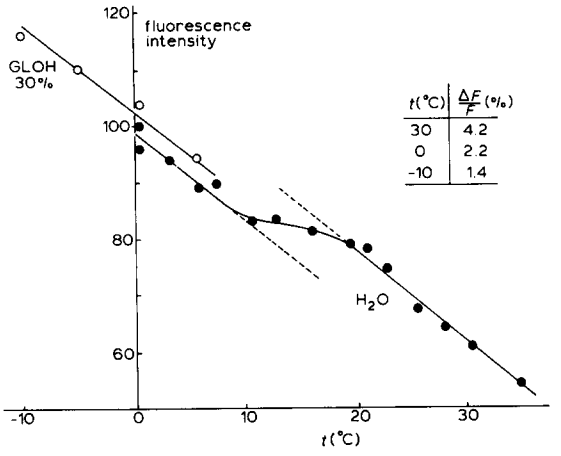

Fig. 2. Temperature dependence of the intensity of tryptophan fluorescence. Measurements were made at pH 7.2 in water (●) or 30% glycerol (GLOH) (○). The relative amplitude of the fluorescence change induced by Ca^{2+} at various temperatures is indicated in the inset.

pletely ruled out. This hypothesis is supported by the studies of Madeen and Quinn [27] who found no difference in cholesterol-enriched membranes and by Dean and Tanford [28] who found the same temperature transition in the activity of detergent solubilized enzyme.

For the present study it was necessary to lower the temperature well below 0°C and the state of the lipid matrix was studied by X-ray diffraction.

The record presented in the fig. 1 shows that a faint 4.2 Å reflection was observable below 0°C in 30% glycerol. The same was true in ethylene glycol. This indicated that a small fraction of the lipids was in a liquid crystalline state. Most of the lipids, however, remained in a disordered conformation even at a temperature as low as −24°C. The temperature range of the transition extends over a range larger than 20 K, as one should expect for an inhomogeneous mixture of lipids.

Fluorescence intensity as a function of temperature

Since the fluorescence intensity of the Ca^{2+} pump protein is strongly dependent on pH [1] the buffer was carefully adjusted to 7.2 at each temperature used.

Up to 10°C the intensity of the fluorescence showed a linear decrease with increasing tempera-

TABLE II

EFFECT OF SOLVENTS ON THE ATPase ACTIVITY

The activity of the ATPase was measured with a pH-stat at 20°C in 100 mM KCl/5 mM $MgCl_2$/5 mM oxalate/1 mM Mg-ATP/100 μM $CaCl_2$/0.5 mM Mops-K (pH 7.2). Titrant was 10 mM KOH. Coupling ratio is calcium transported/ATP cleaved.

Solvent		Measured freezing point (°C)	ATPase activity ($\mu mol \cdot mg^{-1} \cdot min^{-1}$)	Coupling ratio
composition	concentration v/v (%)			
Water	100	0	0.85	1.4
Glycerol/water	10:90	−3.2	0.95	1.3
	20:80	−8	1.1	0.9
	30:70	−14	1.1	0.7
Ethylene glycol/ water	10:90	−4	0.93	1.3
	20:80	−9.5	0.93	1.1
	30:80	−16.5	0.70	0.9
	40:60	−26	0.38	<0.8
Methanol/water	10:90	−5.2	0.93	1.4
	30:80	−11	0.78	<0.6
Ethylene glycol/ methanol/water	10:5:85	−7.6	0.82	1.4
	10:10:80	−13	0.82	1.1
	20:10:70	−24	0.85	1.0

ture. The presence of glycerol had a very limited effect on the enzyme fluorescence (Fig. 2). A pronounced transition was found between 10°C and 20°C. Above 20°C, the points were situated on a line which corresponded to a fluorescence increase of about 10%. The transition between these two domains occurred within about 8°C and was centered at 15°C. This kind of thermal transition has been previously reported for other proteins [29,30] and was generally attributed to thermal denaturation. This was probably not the case here and it is more likely that this break in the temperature dependence of the fluorescence intensity has revealed a thermal structural change which might well be related to the discontinuity in the ATPase activity discussed above.

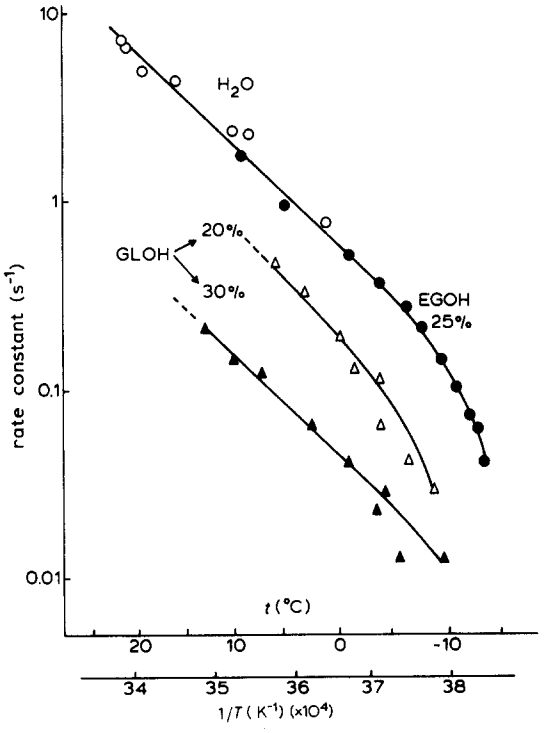

Fig. 3. Arrhenius plot of the rate of the calcium-induced fluorescence change. The rates were measured in the 'on' direction. Vesicles incubated in 50 μM EGTA were mixed with calcium to give a final free calcium concentration of 50 μM. Data in water (○) and ethylene glycol (EGOH) (●) were measured with a stop-flow. Data in glycerol (GLOH) (△,▲) were measured with the stop-flow above 0°C and in a stirred cuvette below 0°C. Other conditions are described in Materials and Methods.

From the experiments presented above it is possible to conclude that, indeed, thermal events can be observed in this protein and in its activity; these events, however, are not clearly related one to another.

The transition observed around 15°C in the protein fluorescence (Fig. 2) has no counterpart either in X-ray spectra (Fig. 1) or in the Arrhenius plot shown in Fig. 3, nor did the freezing of some lipids which occurred below 0°C appear to affect strongly the activation energy of the calcium-induced fluorescence change (Fig. 3) and the protein fluorescence itself (Fig. 2). In addition, cryoprotective solvents like glycerol or ethylene glycol had apparently no effect on the physical state of the lipids and on the activation energy of the fluorescence change although they can modify its rate strongly. It has also been reported recently [6] that, in vesicles, calcium binding at equilibrium was insensitive to the temperature.

Altogether it seems safe to conclude that the mechanism of calcium binding is probably not significantly modified at low temperatures and in the presence of cryoprotective solvents. In the second part of this article the study of the calcium binding mechanism at −10°C in 30% glycerol will be presented. Under these conditions the rate of the calcium-induced transition was nearly three orders of magnitude slower than in water at 20°C (Fig. 3).

(B) Calcium binding at −10°C

Studies at equilibrium

$^{45}Ca^{2+}$ binding at equilibrium was studied by Millipore filtration and the results are shown in Fig. 4a. Similar measurements were made previously at various temperatures [6] and showed a constant number of sites around 6.0 nmol/mg. Data presented here exhibit a clearly cooperative slope ($n_H = 1.6 \pm 0.2$), which was less apparent in the data presented in Ref. 6. The difference resides in the value adopted for the EGTA-Ca stability constant which was taken according to tabulated values [20]; in the present work this constant has been measured and was found significantly smaller. An identical observation was made at pH 6.8 by Ogawa [31].

This uncertainty regarding the EGTA-Ca stabil-

ity constant is a general problem which limits the conclusions which can be derived from the slope of the Ca^{2+}-binding curve of the Ca^{2+}-ATPase.

It can be demonstrated that this is especially crucial at low total calcium concentrations like those used for calcium binding evaluations (50 μM in the present work). Using the various EGTA-Ca stability constants listed in Table I the slope of the binding curve can be significantly modified. The lower values determined by the method described in this work lead to a much steeper curve above 1 μM in addition to an increase of the measured calcium-ATPase dissociation constant.

The fluorescence change as a function of the Ca^{2+} concentration is presented in Fig. 4b. The total EGTA-Ca buffer concentration was kept as low as possible to prevent pH artefacts during the mixing. These effects were also reduced by the use of 50 mM Mops. The data presented in Fig. 4 have been fitted with Scheme III described at the end of this article.

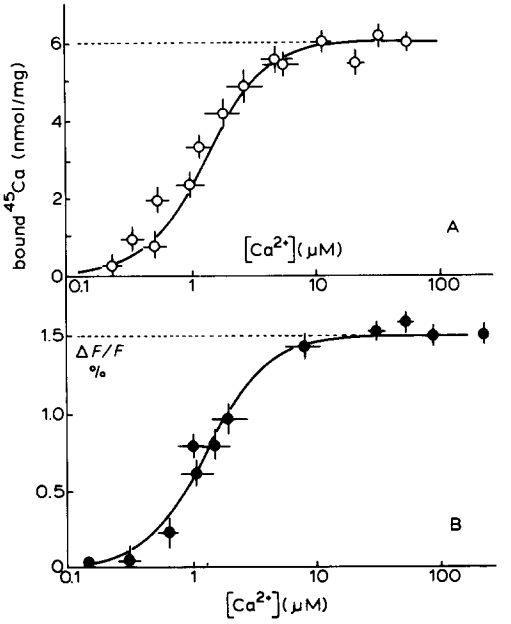

Fig. 4. Titration of high-affinity calcium sites and of the intrinsic fluorescence response. Binding was measured by filtration. The intrinsic fluorescence response was measured as described in Ref. 1. With the same preparation and at the same temperature 3.0 nmol/mg of phosphorylated intermediate were obtained in 5 μM ATP. Temperature was -10°C and solvent contained 30% glycerol. Other reagents were: 100 mM KCl/5 mM $MgCl_2$/50 mM Mops-K, pa_H 7.20. The free calcium concentration as been calculated as described in Methods. Data are fitted using Scheme III and parameters described in the Appendix.

Kinetic studies of fluorescence change and $^{45}Ca^{2+}$ binding at -10°C

Fig. 5 shows typical records of fluorescence changes obtained at -10°C. The range of measurement extends from 20 nM to 150 μM Ca^{2+}, a much wider range than that used in previous kinetic studies [2]. The 'calcium off' rates were measured from 20 nM to 1.0 μM final Ca^{2+} and the 'calcium on' rates from 2.0 to 150 μM Ca^{2+}. The rate constants were estimated by fitting the traces with single exponentials. At high calcium concentrations the 'on' transition showed a deviation from an exponential at the origin. Up to now this fast initial phase has not been correctly resolved and its existence is still uncertain, since it is severaly blurred by mixing and pH artefacts.

The time course of the transition measured by the $^{45}Ca^{2+}$ binding method is shown in Fig. 6. At -10°C and 30% glycerol the shortest time at which binding by filtration could be measured was about 5 s and the complete kinetics were obtained by a variation of the filtration duration. Times were measured to an accuracy of about 2 s.

In 50 μM Ca^{2+} this experiment revealed a net biphasic calcium binding. The rate constant of the fast initial binding could not be obtained since it was completed within the first 10 s after exposure to $^{45}Ca^{2+}$. A slow binding process developed then within minutes and the final binding was always equal to the value found at equilibrium. In 50 μM Ca^{2+} the rate constant of the slow phase was approx. 0.011 s^{-1}. This was identical to the rate constant of the fluorescence change for the same free calcium concentration (see Fig. 5). This experiment therefore indicated that the fluorescence change reflects a major change in the nature or in the accessibility of the Ca^{2+}-binding sites; the mechanism was further investigated by varying the free Ca^{2+} concentration and measuring the amplitudes and rate constants of the fast and slow processes. The range of Ca^{2+} concentration used was 0.3 to 50 μM. The rate constant of the initial burst was always too fast to be measured and its amplitude was evaluated after 10 s filtration in $^{45}Ca^{2+}$ or as described under Fig. 6.

The slow phase of $^{45}Ca^{2+}$ binding was fitted by

a single exponential (Fig. 6B) and the rate constants obtained compared with those obtained by fluorescence. The initial binding was hardly seen below 5 μM Ca^{2+} and should therefore correspond to fast Ca^{2+} binding to a relatively low affinity site. Comparison of the calcium concentration dependence of the amplitude of the early $^{45}Ca^{2+}$ binding (Fig. 7C) with that of the rate constant of the slow binding phase (Fig. 7A) indicated that Ca^{2+} binding to this rapidly accessible low affinity site, was probably responsible for the activation of the rate of the slow calcium binding above 5 μM. The amplitude of the initial burst can be fitted assuming binding to a single site (3 nmol/mg) and a dissociation constant, K_d, of 25 μM.

The rate constants obtained in the fluorescence experiments confirmed the pronounced increase of the 'on' rate above 10 μM which was not completed below 100 μM (Fig. 7A). In addition, a very steep decrease of the 'off' rate was observed above 100 nM (Fig. 7B). Comparison with the binding curve (Fig. 4) showed that these events occurred respectively well above and below the half-saturation of the sites at equilibrium. An analogous observation was made at higher temperature by Guillain et al. [4]. This was not apparent in our earlier studies [2] due to the narrower range of calcium concentrations used.

Measurement of Ca^{2+} exchange at equilibrium

Experiments described here, concern the $^{40}Ca^{2+} \rightleftharpoons {}^{45}Ca^{2+}$ exchange on the high-affinity sites at saturation (50 μM Ca^{2+}). They were performed in both directions and comparable results were obtained (Fig. 8). The exchange showed two phases with one secondary slow rate of release. Data were fitted by two exponentials of equal amplitude with rate constants: $k_{fast} \geq 0.2\ s^{-1}$ and

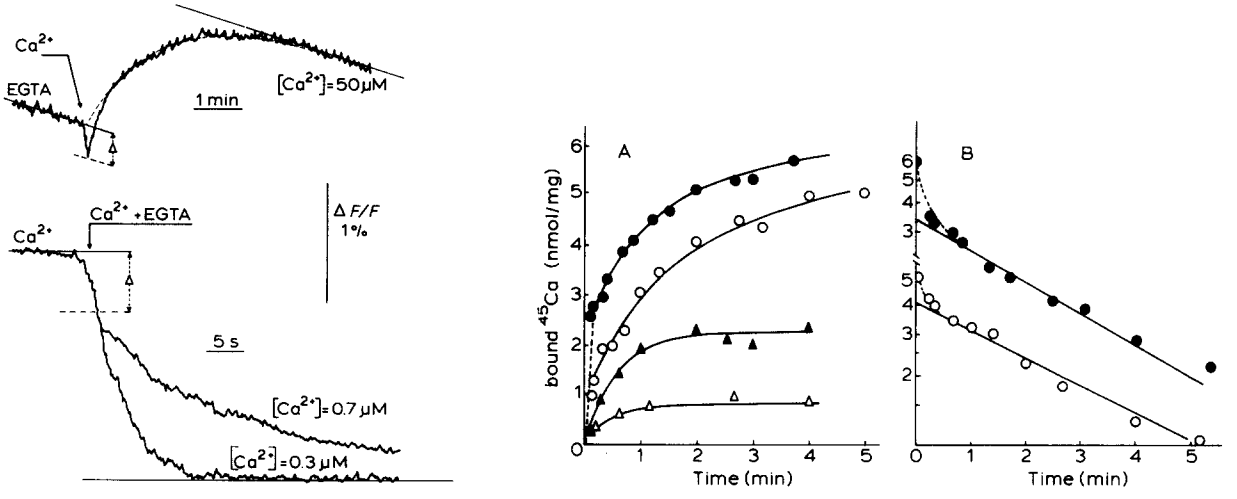

Fig. 5. Time course of the fluorescence change at $-10°C$. In the 'on' direction (above) EGTA concentration was 50 μM. Total calcium added was 100 μM. In the 'off' direction (below) Ca^{2+} concentration before injection was around 10 μM. Solutions injected were Ca-EGTA mixtures. Final concentrations were: Ca^{2+}, 100 μM; EGTA, 120–500 μM. Other reagents are specified under Fig. 4. Δ is the dilution artefact. The slow decrease in fluorescence seen in the upper trace was due to photolysis. The dashed line drawn under the trace is a fit with a single exponential ($k = 0.012\ s^{-1}$).

Fig. 6. Time course of calcium binding. Vesicles were incubated in 250 μM EGTA for several minutes and layered on the Millipore filter (250 μg sample). The filter was then washed during the time indicated with ^{45}Ca/EGTA mixtures to give the indicated free calcium concentrations (μM): $\triangle$, 0.3; $\blacktriangle$, 0.7; ○, 5; ●, 50. (Total $[Ca^{2+}] = 50$ μM.) In B, [(bound $^{45}Ca)_{t=\infty}$ − (bound $^{45}Ca)_t$] was plotted on a logarithmic scale versus filtration time. ○, 5 μM; ●, 50 μM Ca^{2+}. This reveals more clearly two phases of binding. The fast phase was always completed within the first 10 s. For $t > 10$ s, data were fitted with a line giving the rate constant of the slow phase $= 0.011\ s^{-1}$ (●) and $0.009\ s^{-1}$ (○). Extrapolation at $t = 0$ gave the amplitude of the fast phase. Results for various free calcium concentration are given in Fig. 7. Temperature was $-10°C$. Other conditions are as indicated for Fig. 4.

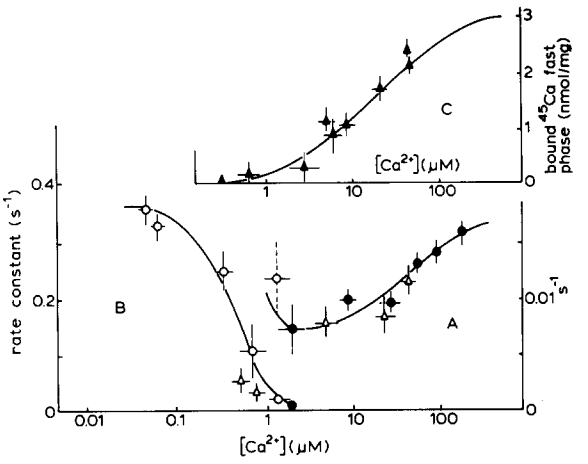

Fig. 7. A and B, Fluorescence change: observed rate constants. They were measured in experiments identical to that described in Fig. 5. Points ○ were measured in the 'off' direction and ● in the 'on' direction. Data △ correspond to the rate constant of the slow phase of calcium binding measured as described in Fig. 6. C. Amplitude of the fast phase of calcium binding. Membranes were incubated in 250 μM EGTA and binding measured as described under Fig. 6. The curve is a fit assuming a saturation at 3 nmol/mg and $K_d = 25$ μM.

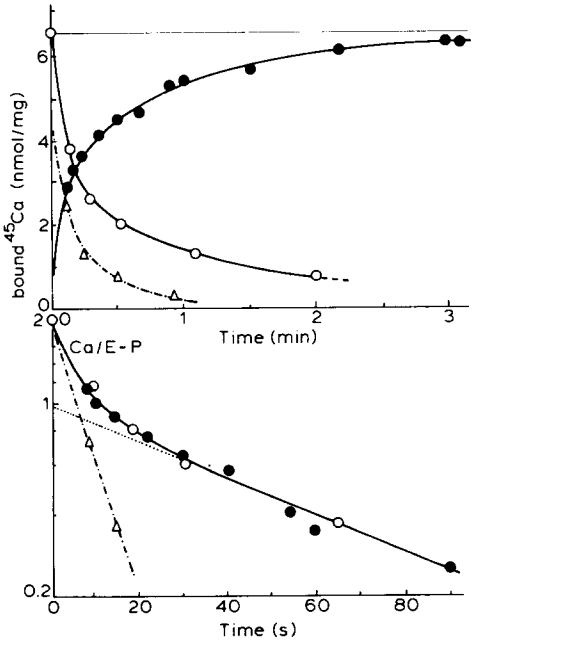

Fig. 8. Calcium isotope exchange at equilibrium. Calcium concentration was 50 μM. ●, $^{40}Ca^{2+} \rightarrow {}^{45}Ca^{2+}$; ○, $^{45}Ca^{2+} \rightarrow {}^{40}Ca^{2+}$; △, $^{45}Ca^{2+} \rightarrow$ EGTA. Data △ were obtained in washing the membranes by 250 μM EGTA. In the semilog plot below, the fraction not exchanged is expressed relative to the phosphorylation site concentration measured in the same sample.

$k_{slow} \approx 0.015\ s^{-1}$. It is likely that k_{fast} was higher than 0.2 s^{-1} since this is the technical limit of the filtration technique used. This experiment showed that, from the rate of exchange at equilibrium, two species of calcium binding site can be revealed.

Kinetics of calcium dissociation

Membranes equilibrated in 50 μM $^{45}Ca^{2+}$ were washed in high [EGTA]. This was different from the exchange experiment described above since dissociated $^{45}Ca^{2+}$ was not replaced. For non-interacting sites one should, however, obtain the same result. This was not the case, and the rate of release of the slow exchanging site was greatly enhanced (0.015 to at least 0.10 s^{-1}) (Fig. 8). The simplest interpretation was that removal of calcium from the fast-exchanging site accelerated the release of Ca^{2+} from the slow one and therefore this experiment was a direct proof of the existence of two classes of interacting Ca^{2+} sites.

Discussion

The dissociation constants of the calcium sites of the sarcoplasmic reticulum calcium pump previously obtained with various techniques using $^{45}Ca^{2+}$ binding range from 0.5 to 1.5 μM [6–12]. This is very close to the K_m for the Ca^{2+} activation of the ATPase [1,13,14] and of the calcium-induced fluorescence change [1,4,12]. Most of these studies were performed in the presence of Ca-EGTA buffer and the variation among the reported values is probably due to the difficulty of the evaluation of the free calcium concentration.

The number of calcium sites is more controversial and values between 6 and 15 nmol/mg were found in sarcoplasmic reticulum vesicles. Considering a molecular weight of 110000 this gives an average of 1–2 calcium sites per polypeptide chain. In the experiments reported here, as in another report at higher temperature [6], we have found 6–7 nmol/mg of high-affinity sites. This was twice the amount in the phosporylated enzyme. The relevance of these binding sites was demonstrated by the fact that nearly all the calcium ions bound at less than 50 μM Ca^{2+} were occluded during phosphorylation and subsequently transported [6]. Furthermore a 2:1 ratio has been also reported many times between the rates of calcium transport

and ATP hydrolysis. Thus, it is more than likely that the transport unit has two high-affinity transport sites. Our binding studies are in favor of one calcium binding site per polypeptide chain *. The same conclusion was reached in two recent reports [11,12].

The binding experiments of Inesi et al. [11] and those of Verjovsky-Almeida et al. [12] are in favor of a high degree of cooperativity between the high affinity calcium sites. This is in agreement with the slope of the binding curve reported here (Fig. 4). However, due to the uncertainties in the evaluation of the free calcium concentrations, this is not sufficient to assert definitively that the two calcium sites are interacting. The analysis of the time course of ^{45}Ca binding and release at low temperature (Figs. 6 and 8) give stronger support for the occurrence of such a mechanism. Measurements reported in Ref. 2, those of Guillain et al. [4] and the work of Inesi et al. [11] were the first attempts to understand the details of the calcium binding mechanism using kinetic and binding data. None of the models proposed, however, is able to fit completely the results described in the present work.

In the first two studies [2,4] the kinetic data are tentatively fitted with the general scheme, Scheme I (see Appendix) which assumes a single class of binding site. With such a scheme, Guillain et al. obtained a reasonably good fit of the rate constants over a very broad range of Ca^{2+} concentration and reproduced the apparent binding constants for calcium at equilibrium. The major drawback of this analysis was that site-site interactions were deliberately neglected, so that $^{45}Ca^{2+}$ binding kinetics and cooperativity cannot be reproduced. On the other hand, the study of Inesi et al. was intended to reproduce correctly the apparent cooperativity of the calcium binding curve. A two-step binding process (Scheme II) was proposed on the basis of fluorescence change kinetic data. With the parameters proposed by the authors it is indeed possible to reproduce the extreme 'off' and 'on' rates, but they are incompatible with the rates measured over a complete range of Ca^{2+} concentration such as those reported by Guillain et al.

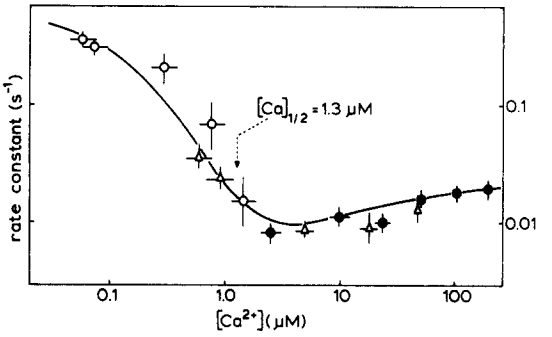

Fig. 9. Simulation of the observed rate constants. Calcium concentration dependence of the rate constants were calculated as described in Appendix (Scheme III). Data and symbols are taken from Fig. 7A, B.

Indeed, it is impossible to make a clear choice between Scheme I and II from the rate constants only, since the equations derived therefrom are identical (See Appendix, Eqns. 2 and 4). It is, for example, possible to fit correctly the rate-constant dependence published by Guillain et al. [4] using sequential binding and a different set of parameters (Guillain et al. personal communication and unpublished data). Another point concerns the very steep reduction of the 'off' rate with increasing calcium concentrations. This is apparent in the data presented by Guillain et al. at pH 7.0 and 5 mM Mg^{2+} and even more clear at $-10°C$ and pa_H 7.2 (Figs. 7, 9). This cannot be fitted correctly assuming that the fluorescence drop after mixing with EGTA is due to the dissociation of calcium from a single class of calcium site. This assumption is made explicitly in Schemes I and II.

The steepness of the calcium concentration dependence of the 'off' rate can be reproduced assuming that dissociation of two calcium ions from interacting sites is necessary for the 'off' fluorescence change to occur. This corresponds to Scheme III in which the two calcium ions are allowed to dissociate directly from the high fluorescent form $E^{\ddagger}$. A set of parameters has been

*The sample used for the binding experiments described in Figs. 4, 6 and 8 was analysed by SDS-polyacrylamide gel electrophoresis. Gels were scanned and gave the following composition: $M_r > 300000$ (possibly ATPase aggregates), 4%; M_r 105000 (ATPase), 65%; M_r 50000–55000, 15%; M_r 44000, 5%; total of other bands, approx. 11%. Titration of around 6 nmol/mg calcium sites is then very close to 1 mol site per ATPase polypeptide chain.

obtained which fits correctly the equilibrium data (Fig. 4) and the Ca^{2+} concentration dependence of the rates (Fig. 9).

Scheme III is the minimum cooperative scheme which is able to simulate correctly the present kinetic and equilibrium data. In this mechanism the two calcium sites are not equivalents. Indeed, filtration experiments at $-10°C$ have indicated that the final state, $E^{\ddagger} \cdot (Ca_1) \cdot (Ca_2)$, was asymmetric with respect to the rate of calcium exchange and also that dissociation of calcium from the slow-exchanging site was accelerated after dissociation of the other calcium ion from the fast exchanging site. This sequential calcium release is included in Scheme III, where dissociation does not occur randomly but via a well-defined sequence.

The most surprising result of this study at low temperature was that one of the two calcium sites was rapidly accessible with a low apparent affinity ($K_d = 25\ \mu M$). According to Scheme III saturation of this site induces the transition $E \rightarrow E^{\ddagger}$ which results (1) in an increase of the apparent affinity of the first site ($K_1 \rightarrow K_1'$) and (2) in the unmasking of the second high-affinity site.

These considerations could lead to a simple model in which the first site has a regulatory role, while the second only is involved in the calcium transport (Scheme III). It is not completely satisfactory, however, since calcium ions bound to the two sites can in fact be occluded and transported after phosphorylation [6]. It is not clear whether such a model can be modified to include the effects of nucleotide binding and phosphorylation.

Yet, another plausible mechanism can be proposed where the asymmetry is only apparent and is created by substrate binding. Koshland et al. [32] showed that cooperativity can be accounted for in assuming sequential conformational changes of the enzyme and formation of hybrid intermediates. In this case the sites are identical and can exist independently in two forms: T, a low-affinity form which is predominant in the absence of ligand; R, a high-affinity form favored by substrate binding. Assuming single ligand and positive cooperativity, the ligand binds first to one subunit and, depending on the type of interaction, this induces a transition to the higher affinity form (R) in the other subunit of the oligomer. The $(T) \rightarrow (R)$ conformational change is a key event in the activation of the enzyme catalytic activity.

In the case of the Ca^{2+}-ATPase, the $(T) \rightarrow (R)$ isomerization should be the transition revealed by the fluorescence change since it is associated with ligand binding and ATPase activation. With respect to the transport mechanism, the most attractive interpretation is that during the $(T) \rightarrow (R)$ transition the change in affinity is accompanied by a change in sidedness of the ion-binding site. Then for two interacting binding sites a more general scheme can be proposed:

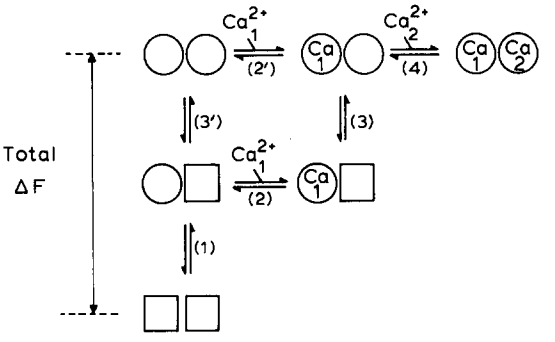

Using the classical representation □ represents the (T) low-affinity state facing the internal space and ○ the (R) high-affinity state facing the cytoplasmic side. Different states of occupancy for external calcium have been represented.

The occupancy of T states by internal calcium has also to be taken into account. The present study was made with relatively low internal calcium concentration (with respect to the expected internal dissociation constant): therefore the T state should be free, but it is clear that the effect of high internal calcium will be an interesting test for this model.

The two calcium sites being equivalent, their affinity for calcium in the R (○) state should now be equally high. The low apparent affinity for the initial binding can be explained by the existence of an unfavorable preexisting fast equilibrium (step 1):

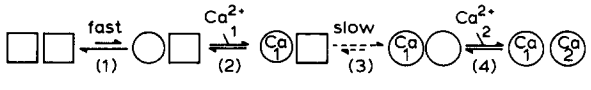

As far as the slow isomerisation (step 3) is concerned, this model is equivalent to Scheme III,

described in the Appendix, steps 1 and 2 being reduced to one low-affinity binding phase of stability constant K_1 (see Appendix).

The process described above can be tested by an investigation of the rate constant of the fast initial $^{45}Ca^{2+}$ binding, but this is presently beyond the possibility of the filtration technique. An important implication of this model is that a hybrid intermediate state (○□) should be detected by fluorescence at high calcium concentrations. Starting from an enzyme in EGTA, the addition of Ca^{2+} induces the following sequence of conformational transitions: □□ → □○ → ○○ and the fluorescence increase should be biphasic. The dead time of the apparatus and the mixing artefacts preclude a detailed analysis of the first stage of the reaction, and the slow isomerization only (step 3) was at present well observed; Fig. 5 shows, however, that there was a net departure from a single exponential when the transition was induced by high calcium.

The nature of the coupling between the calcium sites has not been discussed so far and a subunit-subunit interaction is not strictly necessary for a cooperative interaction. The calcium binding equilibrium data presented here are in favor of one calcium site per polypeptide chain. In this case the observation of a cooperativity implies a subunit-subunit interaction and a minimum dimeric enzyme.

N. Ikemoto [33] and J.P. Froehlich (unpublished data) have observed separately, in multimixing experiments, two distinct families of calcium sites with fast and slow rates of calcium dissociation. Although their experimental conditions were profoundly different from ours, these observations are in good agreement with the biphasic calcium exchange presented in this report. Some of the experiments reported are analogous to the $^{45}Ca \rightarrow$ EGTA chase described in Fig. 8 and demonstrate that the fast dissociation in EGTA is probably also biphasic. This was not clearly observed in the present experiments because of the limited time resolution. The interpretation of these authors is in favor of the existence of two distinct classes of calcium binding site.

Appendix

Scheme I

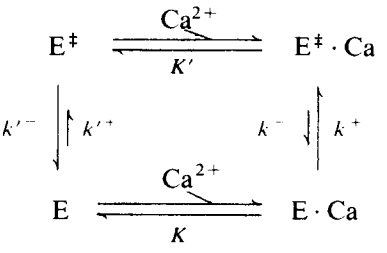

Assuming that calcium is in excess over enzyme and that binding and dissociation are faster than the isomerisation steps. Transition between the two fluorescent forms at a given final calcium concentration [Ca] occurs with an apparent rate:

$$k_{obs} = \frac{k'^{+} + k^{+} \cdot K \cdot [Ca]}{1 + K \cdot [Ca]} + \frac{k'^{-} + k^{-} \cdot K' \cdot [Ca]}{1 + K' \cdot [Ca]} \quad (1)$$

If, as proposed in Refs. 2 and 4, k'^{+} and k^{-} are sufficiently small:

$$k_{obs} \approx \frac{k'^{-}(1 + K \cdot [Ca]) + k^{+} \cdot K \cdot [Ca](1 + K' \cdot [Ca])}{(1 + K \cdot [Ca])(1 + K' \cdot [Ca])} \quad (2)$$

If $k^{+}/k^{-} > 1$, the half-saturation of the site is given by:

$$K_d \approx \frac{1}{K} \cdot \frac{k^{-}}{k^{+}} = \frac{1}{K'} \frac{k'^{-}}{k'^{+}} \quad (3)$$

Scheme II

$$E \underset{K_1}{\overset{Ca_1^{2+}}{\rightleftharpoons}} E \cdot Ca_1 \underset{k^{-}}{\overset{k^{+}}{\rightleftharpoons}} E^{\ddagger} \cdot Ca_1 \underset{K_2}{\overset{Ca_2^{2+}}{\rightleftharpoons}} E^{\ddagger} \cdot Ca_1 \cdot Ca_2$$

This is a sequential binding as proposed by Inesi et al. [11]. If k^{+} and k^{-} are rate limiting:

$$k_{obs} = \frac{k^{-}(1 + K_1[Ca]) + k^{+} \cdot K_1[Ca](1 + K_2[Ca])}{(1 + K_1[Ca])(1 + K_2[Ca])} \quad (4)$$

Writing $K_1 = K$ and $K_2 = K'$, Eqn. 4 is the same as Eqn. 2 which describes Scheme I. The binding curve obtained here is cooperative and half-saturation of the sites is given by:

$$K_d \approx \sqrt{\frac{1}{K_1 \cdot K_2} \cdot \frac{k^{-}}{k^{+}}} \quad (5)$$

Scheme III

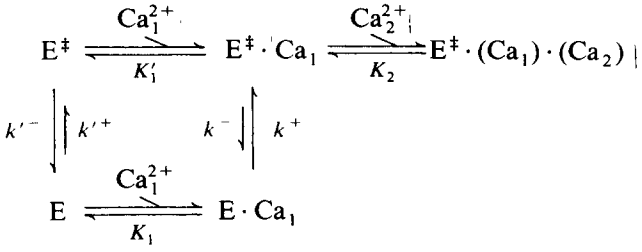

It can be shown that the rate constant for the evolution of such a system is:

$$k_{obs} = \frac{k'^{+} + k^{+} \cdot K_1[Ca]}{1 + K_1[Ca]} + \frac{k'^{-} + k^{-} \cdot K_1'[Ca]}{1 + K_1'[Ca] + K_1' \cdot K_2[Ca]^2} \quad (6)$$

As for Scheme II, the binding is cooperative. If $k^+/k^- > 1$ half-saturation is given by the relation:

$$K_d \approx \sqrt{\frac{1}{K_1 K_2} \frac{k^-}{k^+}} = \sqrt{\frac{1}{K_1' K_2} \frac{k'^-}{k'^+}} \quad (7)$$

The fits of the Figs. 4 and 9 have been calculated with Scheme III and the following set of parameters:
$K_1 = 4 \cdot 10^4\ M^{-1}$
$K_1' = K_2 = 6.7 \cdot 10^6\ M^{-1}$
$k^+ = 0.02\ s^{-1}$ $k'^+ = 0.008\ s^{-1}$
$k^- = 0.009\ s^{-1}$ $k'^- = 0.6\ s^{-1}$

This choice is not unique. The relation $K_1' = K_2$ is made only for symmetry.

Acknowledgements

The author is indebted to N. Ikemoto and J.P. Froehlich for communication of unpublished results and for illuminating discussions and wishes to thank T. Gulik and J.L. Ranck for their help in the X-ray diffraction experiments performed in the 'Centre de Génétique Moléculaire in Gif-s-Yvette. This work is supported by grants from the 'Délégation Générale à la Recherche Scientifique'.

References

1 Dupont Y. (1976) Biochem. Biophys. Res. Commun. 71, 544–550.
2 Dupont Y. and Leigh J.B. (1978) Nature 273, 396–398.
3 Dupont Y. (1978) Biochem. Biophys. Res. Commun. 82, 893–900.
4 Guillain F., Gingold M.P., Büschlen S. and Champeil P. (1980) J. Biol. chem. 255, 2072–2075.
5 Douzou P. (1977) in 'Cryobiochemistry: An Introduction', Academic Press, London
6 Dupont Y. (1980) Eur. J. Biochem. 109, 231–238.
7 Chevalier J. and Butow R.A. (1971) Biochemistry 10, 2733–2737.
8 Meissner G. (1973) Biochim. Biophys. Acta 298, 906–926.
9 Fiehn W. and Migala A. (1971) Eur. J. Biochem. 20, 245–248.
10 Ikemoto N. 91975) J. Biol. Chem. 250, 7219–7224.
11 Inesi G., Kurzmark M., Coan C. and Lewis D.E. (1980) J. Biol. Chem. 255, 3025–3031.
12 Verjovsky-Almeida S. and Silva J.L. (1981) J. Biol. chem. 256, 2940–2944.
13 Makinose M. (1969) Eur. J. Biochem. 10, 74–82.
14 Weber A., Herz R. and Reiss I. 91966) Biochem. Z. 345, 329–369.
15 The R., and Hasselbach W. (1972) Eur. J. Biochem. 28, 357–363.
16 Neet K.E. and Green N.M. (1977) Arch. Biochem. Biophys. 178, 588–597.
17 Hasselbach W. and Makinose M. (1963) Biochem. Z. 339, 94–111.
18 Dupont Y. (1977) Eur. J. Biochem. 72, 185–190.
19 Bennet N. and Dupont Y. (1979) FEBS Lett. 98, 229–232.
20 Bjerrum J., Schwarzenbach G. and Sillen L.G. (1964) in Stability Constants, pp. 697–698, The Chemical Society, London.
21 Portzehl H., Caldwell P.C. and Rüegg J.C. (1964) Biochem. Biophys. Acta 79, 581–591.
22 Hellam D.C. and Podolsky R.J. (1969) J. Physiol. (London) 200, 807–819.
23 Davis D.G., Inesi G. and Gulik-Krzywicki T. (1976) Biochemistry, 15, 1271–1276.
24 Tardieu A., Luzzati V. and Reeman F.C. (1973) J. Mol. Biol. 75, 711–733.
25 Gabriel A. and Dupont Y. (1972) Rev. Sci. Inst. 43, 1600–1602.
26 Inesi G., Millman M. and Eletr S. (1973) J. Mol. Biol. 81, 483–504.
27 Madden T.D. and Quinn P.J. (1979) FEBS Lett. 107, 110–112.
28 Dean W.L. and Tanford C. (1978) Biochemistry 17, 1683–1690.
29 Gally J.A. and Edelman G.M. (1962) Biochim. Biophys. Acta 60, 499.
30 Steiner R.F. and Edelhoch H. (1962) Nature 193, 369.
31 Ogawa Y. (1968) J. Biochem. (Tokyo) 64, 255–257.
32 Koshland and D.E., Nemethy G. and Filmer D. (1965) Biochemistry 5, 365–385.
33 Ikemoto N., Garcia A.M., Kurobe Y. and Scott T.L. (1981) J. Biol. chem. 256, 8593–8601.